3652–3656 *Nucleic Acids Research, 2001, Vol. 29, No. 17*

Characterization of a multi-functional metal-mediated nuclease by MALDI-TOF mass spectrometry

Uraiwan Puapaiboon, Jaran Jai-nhuknan[1] and J. A. Cowan*

Evans Laboratory of Chemistry, The Ohio State University, 100 West 18th Avenue, Columbus, OH 43210, USA and [1]Bruker Daltonics, Inc., 47697 Westinghouse Drive, Fremont, CA 94539, USA

Received April 16, 2001; Revised June 28, 2001; Accepted July 18, 2001

ABSTRACT

Mass spectrometric analysis of reaction products allows simultaneous characterization of activities mediated by multifunctional enzymes. By use of MALDI-TOF mass spectrometry, the relative influence of magnesium and manganese promoted exonuclease and phosphatase activities of *Esherichia coli* exonuclease III have been quantitatively measured, offering a rapid and sensitive alternative to radioactivity quantification and gel electrophoresis procedures for determination of reaction rate constants. Manganese is found to promote higher levels of exonuclease activity, which could be a source of mutagenic effects if this ion were selected as the natural cofactor. Several potential applications of these methods to quantitative studies of DNA repair chemistry are also described.

INTRODUCTION

Exonuclease III is a multifunctional enzyme that mediates exonuclease, RNase H, phosphatase and AP endonuclease activities (1). Among these, the exonuclease and phosphatase activities are of most significance for applications in molecular biology. The enzyme functions as an exonuclease by synchronous 3′–5′ digestion from the 3′-hydroxyl end, and as a phosphatase by cleavage of the 3′-phosphoryl terminus of a double-stranded DNA substrate. Therefore, the products derived from the phosphatase reaction become a new substrate for the exonuclease reaction. Exonuclease activity has previously been assayed either by measuring the release of acid-soluble mononucleotides from ^{32}P-labeled DNA by use of scintillation counting (2), or by gel electrophoresis (3,4). A similar approach has been employed for phosphatase activity by measuring the radioactivity of end-labeled acid-soluble [^{32}P]Pi (inorganic phosphate) fragments released from the substrate (5). A ^{32}P-labeling assay has also been used to quantitate the formation of 3′-phosphate and 3′-phosphoglycolate termini by scintillation counting of bands cut from SDS–polyacrylamide gels (6–9), or by determining band intensity by densitometry (7–9).

In this paper we demonstrate MALDI-mass spectrometry (MS) analysis to be a valuable tool for studies of the kinetics of a multifunctional enzyme such as exonuclease III, allowing direct and simultaneous determination of both exonuclease and phosphatase activities. The resolution afforded by MALDI allows discrimination between phosphorylated and dephosphorylated states of intermediates on important biochemical pathways. The metal ion dependence for exonuclease III activities is also conveniently measured and the influence of Mg^{2+} and Mn^{2+} as enzyme cofactors are compared.

MATERIALS AND METHODS

Both 24mer (5′-GGC CCC CAG GGG CCC CTG GGG GCC-3′) and phosphorylated 24mer (5′-GGC CCC CAG GGG CCC CTG GGG GCC-3′) oligonucleotides were purchased from Integrated DNA Technologies, Inc. (Coralville, IA). 3-Hydroxypicolinic acid (3-HPA), ammonium acetate were purchased from Aldrich (Milwaukee, WI) while cation exchange resin (50 W-X8, mesh size 200–400) was obtained from Bio-Rad (Hercules, CA). Exonuclease III was prepared and purified by standard procedures (10).

A Proflex III (Bruker Daltonics, Inc., Billerica, MA) was used for MALDI-TOF data collection. The instrument is equipped with a 150–200 μJ, 3 ns, N_2 laser (Laser Science, Inc.), a delay-extraction two-stage gridless source, and a two-stage gridless reflectron with a total flight path of 120 cm. The vacuum chamber was held at pressures below 6.0×10^{-6} Torr with a 70 l/s turbo pump. Ions were detected using microchannel plate (Galileo Corp., Sturbridge, MA), and data were recorded on a 1 GHz analog-to-digital converter (LeCroy, Chestnut Ridge, NY) controlled by a Sun workstation (Sun Microsystems, Mountain View, CA). The resolution of the ProFlex instrument is 1000–1500 in the linear mode used here, where resolution is defined as the ratio of the mass (m) to peak width (δm). For the experiments described herein, m ranges from 4000 to 7600 m/z, and δm varies from 4 to 8 m/z in one spectrum.

A double-stranded oligonucleotide substrate was prepared by annealing self-complementary single-stranded 24mer oligonucleotides. Annealing was carried out by heating at 90°C for 10 min in 20 mM Tris–HCl, pH 7.5, and 50 mM NaCl, followed by slow cooling to room temperature. The pelleted double-stranded DNA was obtained by ethanol precipitation

*To whom correspondence should be addressed. Tel: +1 614 292 2703; Fax: +1 614 292 1685; Email: cowan@chemistry.ohio-state.edu
Present address:
Uraiwan Puapaiboon, LumiCyte, Inc., 48480 LakeView Boulevard, Fremont, CA 94538, USA

and allowed to air dry. For exonuclease activity, enzymatic degradation was carried out at room temperature by mixing 12.5 µl of a 0.32 µM exonuclease III solution and 12.5 µl of a solution of 15 µM annealed substrate. The solution buffer for the exonuclease assay consisted of 20 mM Tris–HCl, pH 7.5, 50 mM KCl, 1 mM 2-mercaptoethanol and 8 mM divalent cation (10). The reaction was stopped at the indicated time points by mixing 2 µl aliquots of the assay mix with 1 µl of 3-HPA plus ammonium citrate solution. The resultant mixture was placed into a packed 100-µl pipette tip containing NH_4^+-form cation exchange resin, and eluted by centrifugation at 4000 r.p.m. for 1 min. For MALDI analysis, 0.5 µl of the matrix solution (containing 0.3 M HPA and 0.3 mM ammonium citrate in 25% acetonitrile/water) was deposited onto the sample target disk and air dried (11,12). The purified enzymatic degradation products (0.5 µl) were applied on top of the matrix crystal and allowed to air dry prior to analysis by MALDI-MS. For phosphatase activity, the reaction buffer solution was adjusted to pH 7.0, while other experimental procedures were similar to those described for exonuclease activity.

Kinetic rate constants for the consecutive exonuclease activity were determined by fitting the data to the reaction model using GNUPLOT (http://www.gnuplot.org).

Atomic absorbance measurements were made on a Perkin-Elmer atomic absorption spectrometer using an air/acetylene fuel mixture. The Mg lamp was operated at 285.2 nm, slit width 0.7 mm, and the instrument was calibrated against a series of solutions containing 0.1, 0.3 and 0.5 p.p.m. of Mg^{2+}, prepared by successive dilutions of a 1000 p.p.m. Mg^{2+} standard solution (GFS chemical) with nanopure water that contained 1% cHCl. Volumetric glassware was pretreated with an acid wash. After a preliminary test run, solutions for analysis were diluted to give a concentration <0.5 p.p.m. in the optimal instrumental working range. Both integrated and non-integrated signals were used to determine concentrations of Mg^{2+} to ±2.5%.

RESULTS AND DISCUSSION

Kinetic analysis of phosphatase and exonuclease activities by MALDI-TOF MS analysis

In MALDI-MS analysis, the signal intensity depends on both the power and position of the laser beam on the crystal of the analyte/matrix mixture. The heterogeneity of the cosolidified analyte and matrix mixture leads to variations of the MALDI shot-to-shot and spot-to-spot signals. To minimize such errors in quantitation, an internal standard can be utilized for analyte signal normalization (13,14). This should share many of the physical and chemical properties of the analytes, since different classes of compounds competitively incorporate into the matrix crystal structure and are ionized with differing efficiencies (producing different ion yields). In this present study, all reaction species and degradation products are oligonucleotides or nucleosides, sharing similar structures and compositions. Previous reports support the idea that the optimum internal standard for a specific analyte oligonucleotide is an oligonucleotide with a similar sequence (one base shorter or longer) to that of interest (15,16). We have followed such a protocol in our experiments by measuring the 'relative' intensity (concentration) of oligonucleotides that have similar sequences and differ by only one base. This should assure the accuracy of the experiment when comparing the ratios of the peak intensities of two or more peaks. Combined with careful sample preparation, the signals from analytes with similar structural features should yield constant relative ion intensities that reflect the relative concentration of the analytes.

Table 1. Sequence of oligonucleotide substrate and product fragments

Sequence	Products	Mass
5′-GGC CCC CAG GGG CCC CTG GGG GCC-3′	B	7358
5′-GGC CCC CAG GGG CCC CTG GGG GC3′	C	7069
5′-GGC CCC CAG GGG CCC CTG GGG G-3′	D	6779
5′-GGC CCC CAG GGG CCC CTG GGG-3′	E	6450
5′-GGC CCC CAG GGG CCC CTG GG-3′	F	6121
5′-GGC CCC CAG GGG CCC CTG G-3′	G	5792
5′-GGC CCC CAG GGG CCC CTG-3′	H	5463
5′-GGC CCC CAG GGG CCC CT-3′	I	5133

For a first order reaction A → B defined by rate constant k_1, such as the case for both phosphatase activity and the first step of an exonuclease reaction, the integrated form of the rate equation can be written as

$$[A]_t = [A]_o \exp(-k_1 t)$$

where $[A]_o$ is the concentration of [A] at the starting point, and $[A]_t$ is the concentration of A at time t. At each time point, A is degrading to product B. Therefore, $[A]_o$ is the sum of the species $[A]_t$ and $[B]_t$, which can be written as

$$[A]_o = [A]_t + [B]_t$$

By focusing attention on decay of the reactive species A, a first-order decay profile is obtained. In the general case where more than one product is produced, A → B + C + D ... (see Table 1) then

$$[A]_o = [A]_t + [B]_t + [C]_t + [D]_t + ...$$

Since the relative concentration can be related to the peak intensity and written as

$$[A]_t/[A]_o = I_t/\Sigma I_t$$

where I_t is the intensity of A at time t and ΣI_t is the sum of the intensities at time t, a plot of $\ln([A]_t/[A]_o)$ versus time allows one to determine the rate constant of the reaction, k.

A consecutive reaction model (A → B → C) is used for analysis of the exonuclease activity of a phosphorylated substrate, and the integrated form of the rate equation is defined by

$$[B]_t = k_1([A]_o)[\exp(-k_1 t) - \exp(-k_2 t)]/(k_2 - k_1)$$

where [B] is the concentration of the product of the phosphatase reaction (which is the substrate of the subsequent exonuclease reaction reaction), k_1 is the rate constant for dephosphorylation and k_2 reflects exonuclease activity.

Phosphatase activity

The dependence of exonuclease III catalyzed 3′-dephosphorylation on divalent cations was examined using a 24mer oligonucleotide (Table 1). To reduce complications in data interpretation, the DNA substrate was designed to be self-complementary. In this case, only one series of mononucleotide fragments is observed since the sequences of bases on both strands are the same. Consistent with previously reported work (17–20), only single-stranded DNA fragments were observed. Although exonuclease III is a metal-dependent enzyme, not all metals promote activity equally well and so a study of the effect of the metal cofactor on enzyme activity provides important information concerning the choice of the metals that one should employ to mediate reaction chemistry on double-stranded DNA most efficiently. Herein the rate constants for phosphatase activity mediated by five divalent cations (Mg^{2+}, Mn^{2+}, Ca^{2+}, Sr^{2+} and Ba^{2+}) were determined at a fixed ratio of double-stranded DNA substrate and enzyme concentration. Sequence information for the DNA substrate A is given in Table 1. Only one strand sequence is shown, since the sequence is palindromic.

Low levels of background activity ($k \approx 5.0 \times 10^{-4}$ s^{-1}) were observed in the absence of added divalent cation and reflect the presence of adventitiously bound magnesium cofactor during purification of exonuclease III (21). Atomic absorbance measurements confirmed the presence of approximately 10 atom % of magnesium. Following titration of exonuclease III to 7.5 μM EDTA, the residual activity was completely eliminated. Also, enzyme purified in the the presence of EDTA lacked residual activity.

Figure 1 shows representative mass spectra obtained for the Mg-mediated dephosphorylation reaction at the indicated time points: 1, 2, 4, 8, 10, 15 and 30 min. The peaks at m/z 7438 and 7358 represent the strand with and without the 3′-phosphate end, respectively. Similar data is obtained for Mn-mediated phosphatase activity, and in both cases the phosphatase reaction A → B (Fig. 1, solid line, filled circle) follows a classic first-order reaction profile. Determination of reaction rate constants shows that Mg^{2+} is a slightly more effective cofactor to mediate the cleavage of inorganic phosphate at the 3′-end of double-stranded oligonucleotide followed by Mn^{2+}, with $k_1 \approx 3.6\ (\pm 0.2) \times 10^{-3}$ s^{-1} and $1.6\ (\pm 0.1) \times 10^{-3}$ s^{-1}, respectively (Table 2). Any activity observed for the Ba^{2+}, Sr^{2+} or Ca^{2+} mediated reactions was not above background level. The concentration of metal cofactor used was sufficient to saturate the metal binding site on the enzyme for Mg^{2+}, Mn^{2+} and Ca^{2+} (22). In the case of Ba^{2+} and Sr^{2+} the binding affinity to the enzyme is considerably lower (unpublished results), however, partial activity would have been expected if in fact these two metal ions indeed supported activity. The lack of activity with Ca^{2+} strongly suggests that the larger cations are intrinsically unable to promote enzyme activity.

Since exonuclease III is a multi-functional enzyme, the product was subject to subsequent exonuclease digestion following cleavage of the 3′-phosphate group. This activity is discussed further below.

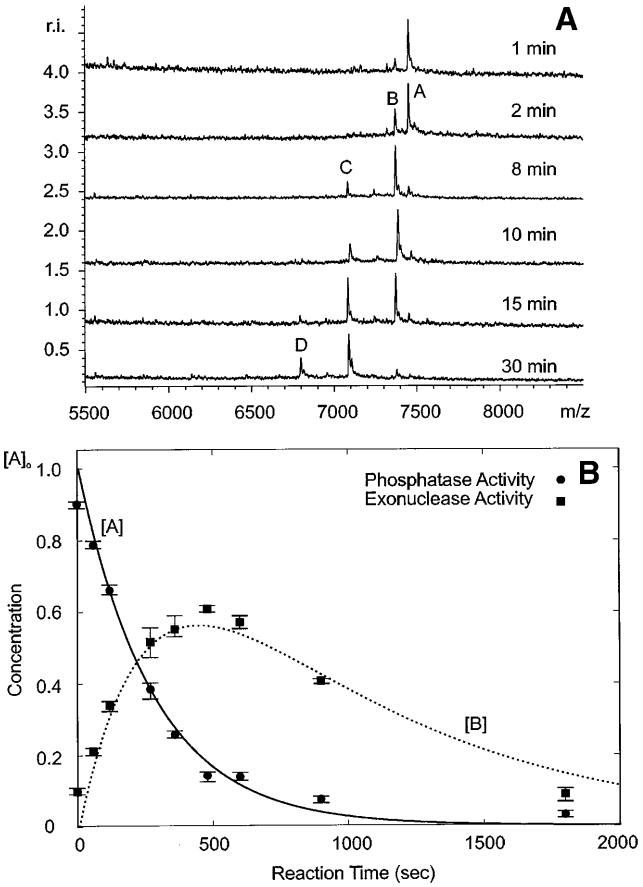

Figure 1. (**A**) MALDI spectra illustrating the time course of the phosphatase and exonuclease activities of *E.coli* exonuclease III mediated by Mg^{2+}. The relative intensity (r.i.) of peaks of defined masses is shown through a series of spectra taken at 0, 1, 2, 4, 8, 15 and 30 min from the top to the bottom, respectively, after mixing the sample. A represents the peak of 24mer single-stranded oligonucleotide (only single-stranded oligonucleotide was observed, see text) containing the 3′-phosphoryl group, and B indicates the mass peak following loss of the phosphoryl group. C and D represent peaks from products following exonuclease activity after the dephosphorylation step. (**B**) Time-dependence of the fractional concentrations of A and B, which vary as a result of dephosphorylation and exonuclease activity. Data for the exonuclease activity were fit to a model for a consecutive reaction using GNUPLOT (http://www.gnuplot.org). Data for the phosphatase were fit to a standard first-order decay curve.

Table 2. Metal ion-dependence of the rate constants for exonuclease and phosphatase activities of *E.coli* exonuclease III

Metal cofactor	k_1 (s^{-1})	k_2 (s^{-1})	k_{EXO} (s^{-1})
Mg^{2+}	$3.6\ (\pm 0.2) \times 10^{-3}$	$1.3\ (\pm 0.2) \times 10^{-3}$	$4.7\ (\pm 0.5) \times 10^{-3}$
Mn^{2+}	$1.6\ (\pm 0.1) \times 10^{-3}$	$1.6\ (\pm 0.1) \times 10^{-3}$	$17\ (\pm 2) \times 10^{-3}$

k_1 is the rate constant for phosphatase activity, k_2 is the rate constant for exonuclease activity determined from a consecutive reaction model and k_{EXO} is the exonuclease activity determined from a non-phosphorylated substrate.

Exonuclease activity

The rate constants for exonuclease activity mediated by Mg^{2+} and Mn^{2+} were determined at a fixed ratio of dephosphorylated double-stranded DNA substrate and enzyme concentration, and followed a strategy similar to that described earlier for phosphatase activity. Sequence information for the DNA

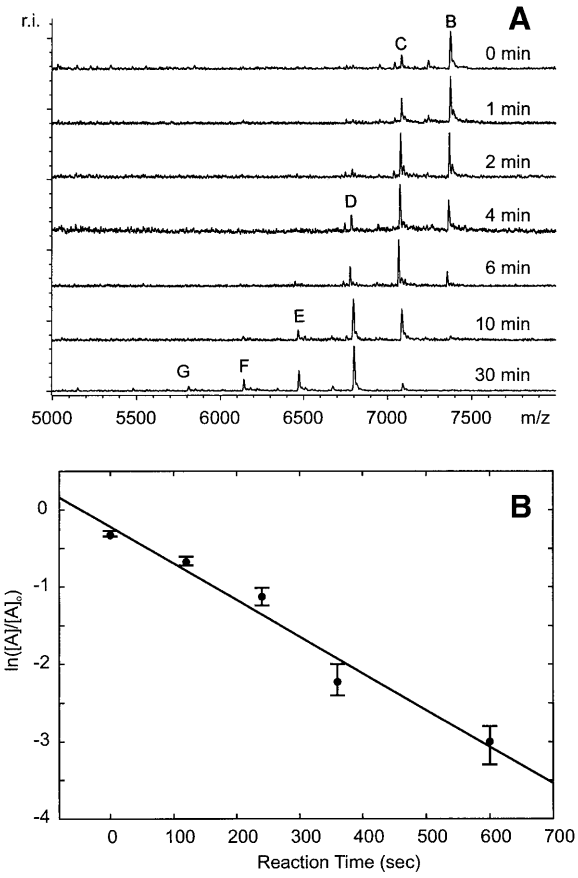

Figure 2. (**A**) MALDI spectra illustrating the time course of the exonuclease activity of *E.coli* exonuclease III mediated by Mg^{2+}. The relative intensity (r.i.) of peaks of defined masses is shown through a series of spectra taken at 0, 1, 2, 4, 8, 15 and 30 min from the top to the bottom, respectively, after mixing the sample. B, C, D, E, F and G represent the peaks of the reaction products from exonuclease activity as described in Table 1. (**B**) Determination of the observed rate constant for exonuclease activity mediated by Mg^{2+}, from a plot of $\ln[B]/[B]_o$ versus time.

substrate A, and the enzymatic degradation products B–I are illustrated in Table 1. Only one strand sequence is shown, since the sequence is palindromic. Figure 2 shows data for Mg^{2+}-promoted exonuclease activity (following peak A) of a non-phosphorylated substrate. The intrinsic phosphatase and exonuclease activities appear to be closely matched for Mg^{2+} cofactor (with rate constants of 3.6×10^{-3} s^{-1} and 4.7×10^{-3} s^{-1}, respectively), but differing by an order of magnitude (1.6×10^{-3} s^{-1} versus 17×10^{-3} s^{-1}, respectively) for Mn^{2+}-promoted activity. This observation has significance for DNA repair pathways following DNA damage from chemical and physical agents such as H_2O_2, ionizing radiation, and neocarzinostatin and bleomycin antibiotics. These produce a variety of lesions, including formation of apurinic/apyrimidinic (AP) sites. Rapid exonuclease cleavage following dephosphorylation can cause problems during repair synthesis by DNA polymerase, which fills the gap across an AP site, with the consequent high probability of creating a mutagenic site (23). The selection of Mg^{2+} circumvents such a problem.

Exonuclease activity of a phosphorylated substrate has also been considered and modeled assuming a consecutive reaction pathway as described earlier. Figure 1 shows data obtained for Mg^{2+}-mediated exonuclease activity at the indicated time points (0, 1, 2, 4, 8, 15 and 30 min, respectively). By subtracting the peak intensity of each peak from that of the baseline prior to plotting $\ln([B]_t/[B]_o)$ versus time, rate profiles were obtained for the exonuclease reaction B $\rightarrow$ C (Fig. 1, dashed line, filled square). The concentration of B was observed to reach a maximum at ~500 s indicating that it is an intermediate of a consecutive reaction. For other divalent cations, the same approach was applied and the results are summarized in Table 2. The effect of divalent cations on the enhancement of the exonuclease activity of exonuclease III can be written in the order of $Mn^{2+} > Mg^{2+} >> Ba^{2+} \sim Ca^{2+} \sim Sr^{2+} \sim$ blank, and shows a dramatic variation in the rate of digestion when a 24mer self-complementary double-stranded DNA substrate was treated with exonuclease III in the presence of each of the added divalent cations.

The rate of exonuclease digestion following the dephosphorylation step was found to be slower than that of exonuclease activity alone (see Table 2), and was the same as that obtained for the phosphatase activity, within the margin of error of the measurements. This result is consistent with rate-limiting dephosphorylation. Also of significance is the observation that the manganese-promoted dephosphorylation pathway shows significant exonuclease activity, with loss of the first mononucleotide (peak at m/z = 7069) after only half of the sample had been dephosphorylated.

A comparison of previously reported activity data for exonuclease function (5,10) shows remarkable consistency with the results determined here following correction for variation in definitions of substrate concentration (base pair versus individual strand). The enhanced activity of Mn^{2+} relative to Mg^{2+} promoted reactions is also consistent with prior results on a variety of nuclease enzymes (24).

Finally, our finding that the larger Ca^{2+}, Ba^{2+} and Sr^{2+} ions do not promote either activity is consistent with findings for other Mg-dependent enzymes. The distinct chemistry of the larger ions (22,24) appears to preclude their use as efficient catalysts. Even though Ca^{2+} binds strongly to exonuclease III (22), it appears to lack either sufficient Lewis acidity and/or structural organization ability to promote activities from exonuclease III (sic Ba^{2+} and Sr^{2+}). The natural magnesium cofactor is found to be optimal, although not necessarily the most effective cofactor, for biologically relevant chemistry. As described earlier the rapid exonuclease activity of the Mn^{2+}-promoted enzyme can be a source of mutagenic effects, and so we learn how nature circumvents such a problem through selection of the metal cofactors that minimize, and promote the repair of such damage.

CONCLUSIONS

MALDI-TOF MS is demonstrated to be an efficient tool with which to study the influence of metals on the phosphatase and exonuclease activities of exonuclease III. Success in efficient cleaning of sample mixtures containing divalent cation species, an essential requirement for activity in these enzymatic reactions, has allowed us to formulate a new approach for determination of the rate constants of these reactions.

MALDI-TOF MS analysis is here demonstrated to provide a rapid and sensitive approach that can be used to replace conventional methods such as radioactivity quantification and gel electrophoresis. Moreover, it provides simultaneous monitoring of two or more reaction pathways that are mediated by the same multifunctional enzyme. This has been demonstrated through studies of the metal dependence of exonuclease and phosphatase activities of exonuclease III.

Complementary to such experiments are related applications for quantitative studies of DNA repair chemistry. Chemical and physical agents that damage DNA (such as H_2O_2, ionizing radiation, and neocarzinostatin and bleomycin antibiotics) produce a variety of lesions (25,26). These include single- and double-strand breaks, base modifications and formation of AP sites. Since it is difficult to study the repair pathways for all of these lesions in a single experiment, previous efforts to study these types of repair reaction have used distinct assays for each (8,27,28). Herein we have demonstrated MALDI-TOF MS to be suited to characterization and quantification of multiple reaction products in a single experiment by direct mass measurement. The ability to characterize and quantify the products of DNA lesions and the reaction profiles of multifunctional enzymes by use of MALDI-TOF MS will expedite our understanding of these biological reactions.

ACKNOWLEDGEMENTS

This work was supported by grants from the National Science Foundation (CHE-0111161) and the Petroleum Research Fund, administered by the American Chemical Society.

REFERENCES

1. Rogers,S.G. and Weiss,B. (1980) Exonuclease III of *Escherichia coli* K-12 and AP endonuclease. *Methods Enzymol.*, **65**, 203–231.
2. Richardson,C.C. and Kornberg,A. (1964) Enzymic synthesis of deoxyribonucleicc acid. Purification and properties of deoxyribonucleic acid polymerase. *J. Biol. Chem.*, **239**, 240–250.
3. Hoheisel,J.D. (1993) On the activities of *Escherichia coli* exonucleases III. *Anal. Biochem.*, **209**, 238–246.
4. Roychoudhury,R. and Wu,R. (1977) Novel properties of *Escherichia coli* exonuclease III. *J. Biol. Chem.*, **252**, 4786–4789.
5. Milcarek,C. and Weiss,B. (1972) Mutants of *Escherichia coli* with altered deoxyribonucleases. I. Isolation and characterization of mutants for exonuclease III. *J. Mol. Biol.*, **68**, 303–318.
6. Henner,W.D., Grunberg,S.M. and Haseltine,W.A. (1983) Enzyme action at 3′ termini of ionizing radiation-induced DNA strand breaks. *J. Biol. Chem.*, **258**, 15198–15205.
7. Bertoncini,C.R.A. and Meneghini,R. (1995) DNA strand breaks produced by oxidative stress in mammalian cells exhibit 3′-phosphoglycolate termini. *Nucleic Acids Res.*, **23**, 2995–3002.
8. Winters,T.A., Russell,P.S., Kohli,M., Dar,M.E., Neumann,R.D. and Jorgensen,T.J. (1999) Determination of human DNA polymerase utilization for the repair of a model ionizing radiation-induced DNA strand break lesion in a defined vector substrate. *Nucleic Acids Res.*, **27**, 2423–2433.
9. Kappen,L.S., Chen,C.-Q. and Goldberg,I.H. (1988) Atypical abasic sites generated by neocarzinostatin at sequence-specific cytidylate residues in oligodeoxynucleotides. *Biochemistry*, **27**, 4331–4340.
10. Black,C.B. and Cowan,J.A. (1997) Inert chromium and cobalt complexes as probes of magnesium dependent enzymes. Evaluation of the stoichiometry and mechanistic role of the essential metal cofactor in *E. coli* exonuclease III. *Eur. J. Biochem.*, **243**, 684–689.
11. Puapaiboon,U., Jai-nhuknan,J. and Cowan,J.A. (2000) Rapid and direct sequencing of double-stranded DNA using exonuclease III and MALDI-TOF MS. *Anal. Chem.*, **72**, 3338–3341.
12. Little,D.P., Cornish,T.J., O'Donnell,M.J., Braun,A., Cotter,R.J. and Koster,H. (1997) MALDI on a chip: analysis of arrays of low-femtomole to subfemtomole quantities of synthetic oligonucleotides and DNA diagnostic products dispensed by a piezoelectric pipet. *Anal. Chem.*, **69**, 4540–4546.
13. Bruenner,B.A., Yip,T.T. and Hutchens,T.W. (1996) Quantitative analysis of oligonucleotides by matrix-assisted laser desorption/ionization mass spectrometry. *Rapid Commun. Mass Spectrom.*, **10**, 1797–1801.
14. Bleczinski,C.F. and Richert,C. (1998) Monitoring the hybridization of the components of oligonucleotide mixtures to immobilized DNA via matrix-assisted laser desorption/ionization time-of-flight mass spectrometry. *Rapid Commun. Mass Spectrom.*, **12**, 1737–1743.
15. Houston,C.T., Taylor,W.P., Widlanski,T.S. and Reilly,J.P. (2000) Investigation of enzyme kinetics using quench-flow techniques with MALDI-TOF mass spectrometry. *Anal. Chem.*, **72**, 3311–3319.
16. Zhang,L.-K. and Gross,M.L. (2000) Matrix-assisted laser desorption/ionization mass spectrometry methods for oligodeoxynucleotides: improvements in matrix, detection limits, quantification and sequencing. *J. Am. Soc. Mass Spectrom.*, **11**, 854–865.
17. Liu,Y.H., Lubman,D.M. and Venta,P.J. (1995) Use of a nitrocellulose film substrate in matrix-assisted laser desorption/ionization mass spectrometry for DNA mapping and screening. *Anal. Chem.*, **67**, 3482–3490.
18. Siegert,C.W., Jacob,A. and Köster,H. (1996) Matrix-assisted laser desorption/ionization time-of-flight mass spectrometry for the detection of polymerase chain reaction products containing 7-deazapurine moieties. *Anal. Biochem.*, **243**, 55–65.
19. Doktycz,M.J., Hurst,G.B., Habibi-Goudazi,S., McLuckey,S.A., Tong,K., Chen,C.H., Vziel,M., Jacobson,K.B., Woychik,R.P. and Buchanan,M.V. (1995) Analysis of polymerase chain reaction-amplified DNA products by mass spectrometry using matrix-assisted laser desorption and electrospray: current status. *Anal. Biochem.*, **230**, 205–214.
20. Benner,W.H., Horn,D., Katz,J. and Jaklevic,J. (1995) Identification of denatured double-stranded DNA by matrix-assisted laser desorption/ionization time-of-flight mass spectrometry. *Rapid Commun. Mass Spectrom.*, **9**, 537–540.
21. Demple,B., Johnson,A. and Fung,D. (1986) Exonuclease III and endonuclease IV remove 3′ blocks from DNA synthesis primers in hydrogen peroxide-damaged *Escherichia coli*. *Proc. Natl Acad. Sci. USA*, **83**, 7731–7735.
22. Casareno,R.L.B. and Cowan,J.A. (1996) Magnesium versus manganese cofactors for metallonuclease enzymes. A critical evaluation of thermodynamic binding parameters and stoichiometry. *Chem. Commun.*, 1813–1814.
23. Loeb,L.A. and Preston,B.D. (1986) Mutagenesis by apurinic/apyrimidinic sites. *Annu. Rev. Genet.*, **20**, 201–230.
24. Cowan,J.A. (1998) Metal activation of enzymes in nucleic acid biochemistry. *Chem. Rev.*, **98**, 1067–1088.
25. Teebor,G.W., Boorstein,R.J. and Cadet,J. (1988) The repairability of oxidative free radical mediated damage to DNA: a review. *Int. J. Radiat. Biol.*, **54**, 131–150.
26. Demple,B. and Harrison,L. (1994) Repair of oxidative damage to DNA: enzymology and biology. *Annu. Rev. Biochem.*, **63**, 915–948.
27. Takemoto,T., Zhang,Q.-M., Matsumoto,Y., Mito,S., Izumi,T., Ikehata,H. and Yonei,S. (1998) 3′-Blocking damage of DNA as a mutagenic lesion caused by hydrogen peroxide in *Escherichia coli*. *J. Radiat. Res. (Tokyo)*, **39**, 137–144.
28. Karimi-Busheri,F., Lee,J., Tomikson,A.E. and Weinfeld,M. (1998) Repair of DNA strand gaps and nicks containing 3′-phosphate and 5′-hydroxyl termini by purified mammalian enzymes. *Nucleic Acids Res.*, **26**, 4395–4400.